Available online at www.sciencedirect.com
SCIENCE DIRECT
Biochimica et Biophysica Acta 1712 (2005) 17 – 28
BIOCHIMICA ET BIOPHYSICA ACTA
BBA
http://www.elsevier.com/locate/bba

Studies on canthaxanthin in lipid membranes

Agnieszka Sujak[a,b], Janina Gabrielska[c], Justyna Milanowska[a], Piotr Mazurek[d], Kazimierz Strzałka[e], Wiesław I. Gruszecki[a,*]

[a]Department of Biophysics, Institute of Physics, Maria Curie-Skłodowska University, 20-031 Lublin, Poland
[b]Department of Physics, Agricultural University, 20-033 Lublin, Poland
[c]Department of Physics and Biophysics, Agricultural University, Wrocław, Poland
[d]Department of Surface Physics and Nanostructures, Institute of Physics, Maria Curie-Skłodowska University, 20-031 Lublin, Poland
[e]Department of Plant Physiology and Biochemistry, Faculty of Biotechnology, Jagiellonian University, Kraków, Poland

Received 23 November 2004; received in revised form 18 March 2005; accepted 24 March 2005
Available online 11 April 2005
Dedicated to Prof. S. Przestalski

Abstract

Polar carotenoid pigment – canthaxanthin – has been found to interfere with the organization of biological membranes, in particular of the retina membranes of an eye of primates. The organization of lipid membranes formed with dipalmitoylphosphatidylcholine (DPPC) and egg yolk phosphatidylcholine containing canthaxanthin was studied by means of several techniques including: electronic absorption spectroscopy, linear dichroism, X-ray diffractometry, ^{1}H-NMR spectroscopy and FTIR spectroscopy. It appears that canthaxanthin present in the lipid membranes at relatively low concentration (below 1 mol% with respect to lipid) modifies significantly physical properties of the membranes. In particular, canthaxanthin (i) exerts restrictions to the segmental molecular motion of lipid molecules both in the headgroup region and in the hydrophobic core of the bilayer, (ii) promotes extended conformation of alkyl lipid chains, (iii) modifies the surface of the lipid membranes (in particular in the gel state, L'_β) and promotes the aggregation of lipid vesicles. It is concluded that canthaxanthin incorporated into lipid membranes is distributed among two pools: one spanning the lipid bilayer roughly perpendicularly to the surface of the membrane and one parallel to the membrane, localized in the headgroup region. The population of the horizontal fraction increases with the increase in the concentration of the pigment in the lipid phase. Such a conclusion is supported by the linear dichroism analysis of the oriented lipid multibilayers containing canthaxanthin: The mean angle between the dipole transition moment and the axis normal to the plane of the membrane was determined as 20±3° at 0.5 mol% and 47±3° at 2 mol% canthaxanthin. The analysis of the absorption spectra of canthaxanthin in the lipid phase and ^{1}H-NMR spectra of lipids point to the exceptionally low aggregation threshold of the pigment in the membrane environment (~1 mol%). All results demonstrate a very strong modifying effect of canthaxanthin with respect to the dynamic and structural properties of lipid membranes.

Keywords: Canthaxanthin; Biomembrane; Carotenoid pigment; Lipid membrane; Molecular aggregation; Retinopathy

1. Introduction

Carotenoids, the most widespread naturally occurring pigments, are considered essential in several important biological processes, such as the regulation of membrane fluidity [1,2], antennae and photoprotection functions in photosynthesis or other light-induced biological processes [2–5]. Over the last decades, many of carotenoid pigments are used widely in food industry and cosmetics as pigments giving an attractive color [6] and functioning as anti-oxidants [7–11]. Although they are generally evaluated as non-harmful, many cases show that their usage can lead to the organism pathologies.

Canthaxanthin (CAN) has been studied extensively in recent times, mainly because its application as a food

Abbreviations: CAN, canthaxanthin; DPPC, dipalmitoylphosphatidylcholine; EYPC, egg yolk phosphatidylcholine; NMR, nuclear magnetic resonance; PCS, photon correlation spectroscopy; FTIR, Fourier transform infrared absorption spectroscopy

* Corresponding author. Fax: +48 81 537 61 91.
E-mail address: wieslaw@tytan.umcs.lublin.pl (W.I. Gruszecki).

0005-2736/$ - see front matter © 2005 Elsevier B.V. All rights reserved.
doi:10.1016/j.bbamem.2005.03.010

colorant and a component of tanning creams and pills [12]. In spite of the reported anti-cancer [13], anti-tumor or anti-dermatosis [14,15] abilities of this molecule, there is a growing body of literature on the effects of canthaxanthin and other carotenoids in human chronic diseases including canthaxanthin retinopathy [16–25], retinal dystrophy [26] or aplastic anemia [27,28]. Many studies on animals [28–30] and a human case reports [16–22,24,26] communicate the formation of canthaxanthin crystals within the membranes of the *macula lutea* both after or without using high doses of this colorant in a diet or as a tanning agent [15,16,19,28]. Together with a *macula* dysfunction no functional impairment of the membrane or body has been detected [30]. On the contrary, it has been suggested that the process of developing crystals can be due to a metabolic defect in canthaxanthin metabolism, some pre-existing changes in the retinal pigments [29] or the existence of pre-disposing factors [23]. Interactions of CAN and lipid molecules in lipid membranes seem to play a key role in many of the biological effects of this carotenoid pigment. In this study, we address the problem of the effect of canthaxanthin on the physical properties of lipid membranes.

2. Materials and methods

2.1. Chemicals

Dipalmitoylphosphatidylcholine (DPPC) and egg yolk phosphatidylcholine (EYPC) were purchased from Sigma Chem Co. (USA). Synthetic, crystalline canthaxanthin (β,β-carotene-4,4′-dione) was purchased from Fluka (Switzerland). Chemicals were stored under argon in a deep-freezer. Directly before use, canthaxanthin was re-purified by means of HPLC technique (column length 250 mm, internal diameter 4.6 mm, filled with Nucleosil C-18). The solvent mixture acetonitrile:methanol (72:8, v:v) was used as a mobile phase. The molar concentration of CAN used was evaluated spectrophotometrically using the molar extinction coefficients from the literature [5].

2.2. Preparation of small unilamellar liposomes containing incorporated canthaxanthin

Small unilamellar liposomes for spectroscopic measurements were prepared as described in detail previously [31]. Briefly, the vacuum-dried thin film of DPPC and CAN mixture in a glass tube was hydrated with 10 mM Tricine buffer, pH 7.6 and vigorously vortexed at 45 °C for 10 min. The final lipid concentration in the liposome suspensions was 0.2 mg/ml. The homogenous suspension was then subjected to sonication for 2 min with a 20 kHz ultrasonic disintegrator (Unipan) equipped with a titanium probe, at the temperature (45 °C) maintained above the main phase transition of DPPC. The small unilamellar liposome suspensions were centrifugated at 15,000×*g* to eliminate pigment microcrystals possibly non-incorporated into the membranes [31,32].

2.3. Liposome preparation and NMR measurements

Small unilamellar DPPC vesicles for NMR measurements were prepared as described previously [33]. In brief, the lipid with an appropriate amount of canthaxanthin was mixed in chloroform. After removing solvent, the dry lipid film was hydrated with D_2O. The final concentration of lipid was 25 mg/ml. The concentrations of canthaxanthin were 0.24, 0.6, 1.0, 1.5 and 3.7 mol% with respect to the lipid. The suspensions were then sonicated under nitrogen for 30 min with a 20 kHz sonicator equipped with a titanium probe. During the sonication, the samples were thermostated at 55 °C, above the main phase transition temperature of DPPC. The sonication was followed by the centrifugation for 5 min at 2000×*g* in order to remove possible titanium particles. The NMR spectra of 0.5-ml samples of vesicle suspension supplemented with 4.09 mM $PrCl_3$ in 5-mm NMR tubes were collected. The ratio of the $-N(CH_3)_3$ downfield signal to the upfield signal after the addition of $PrCl_3$ was approximately 1.3.

^{1}H-NMR spectra were recorded on Bruker Avance DRX spectrometer. 300 MHz ^{1}H-NMR parameters were as follows: spectral window 6173 Hz; digital resolution 0.188 Hz; pulse width 4.5 μs (30° flip angle); acquisition and delay times were 2.65 s and of 1 s, respectively; and acquisition temperature 48 °C.

2.4. Electronic absorption spectroscopy, linear dichroism measurements and X-ray diffractometry

Absorption spectra were recorded with a double beam UV–Vis 160A-PC spectrophotometer equipped with thermostated cell holders. Experiments were carried out in the temperature range from 10 °C to 50 °C. A constant temperature during the recording of spectra was controlled with a Poly Science thermostated circulator and the temperature in the cuvette monitored with NiCl–NiAl thermocouple. During the experiments, the liposome suspension was stirred with a magnetic microstirrer. Non-pigmented DPPC liposomes were used as a reference. Absorption spectra were recorded every 3 °C except the region of the main phase transition (around 41 °C) in which the spectra were recorded every 1 °C. Diffractometric measurements were performed according to the method described in detail previously [35]. The oriented multibilayers deposited to the glass support consisted of 100 single bilayers. Θ–2Θ X-ray measurements were performed with a HZG4 diffractometer equipped with a copper anode and a nickel filter.

The linear dichroism measurements of the orientation of canthaxanthin molecules in the lipid membranes were performed also in the oriented lipid multilayers deposited

to the glass support, composed of 50 bilayers, the same as prepared for the diffractometric measurements, containing 0.5 and 2 mol% canthaxanthin. Polarized light absorption spectra were recorded with UV–Vis Shimadzu 160A-PC spectrophotometer equipped with the Shimadzu polarizing attachment. The dichroic ratio was determined at 470 nm and the orientation of the dipole transition moment of CAN with respect to the axis normal to the plane of the membrane was calculated as described in detail previously [34].

2.5. Infrared absorption measurements and photon correlation spectroscopy liposome size measurements

Infrared absorption spectra were recorded with a Fourier transform infrared spectrophotometer (FTIR) from Bruker Optik (Germany) model Vector 33, equipped with a horizontal attenuated total reflection (ATR) cell. Spectra were recorded with a resolution of 0.6 cm^{-1}. In order to record FTIR spectra, liposomes of DPPC, containing CAN or formed with the pure lipid, were deposited to ZnSe crystal as a hydrated lipid multibilayer.

Liposome size distribution was determined using photon correlation spectroscopy (PCS). The measurements were performed using EYPC and DPPC liposome suspensions in PBS buffer of pH 7.0. Unilamellar liposomes were obtained by ten-fold extrusion of lipid dispersion (containing appropriate amount of canthaxanthin) through polycarbonate filter (pore size 100 nm). In the case of DPPC liposomes, the extrusion procedure was done at 50 °C, whereas EYPC liposomes were prepared at room temperature. The lipid concentration in the liposome suspension was 1.32 mM. The concentrations of canthaxanthin were 0.1, 0.5, 1.0, 2,0 and 5.0 mol% with respect to the lipid. For the measurements, 30 μl of liposome suspension was diluted to a final volume of 2 ml PBS buffer. PCS measurements were carried out at room temperature (20 °C, for EYPC liposomes) and at 20 °C and at 50 °C (for DPPC vesicles) in 1 cm cuvette on a Zetasizer 5000 instrument (Malvern Instruments Ltd, UK). A laser light of 635 nm, scattered by the sample, was amplified and then analyzed by a correlator to obtain a correlation function, which shape depended on size of the liposomes in the sample.

3. Results and discussion

Fig. 1 presents the electronic absorption spectra of canthaxanthin (CAN) in selected organic solvents. The spectra in the region between 400 nm and 550 nm correspond to the electronic transition between the ground energy level ($1A_g^-$) and the B_u^+ state. Similarly to the other carotenoid pigments substituted with keto groups at the 4 and/or 4′ position, such as astaxanthin, the absorption spectra of CAN recorded at room temperature do not display vibronic substructure typical of other polar carotenoids [5]. CAN incorporated into model lipid membranes, liposomes,

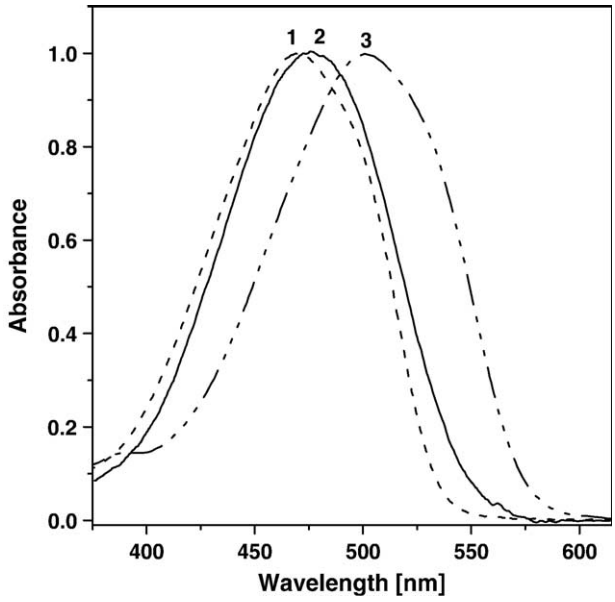

Fig. 1. Normalized electronic absorption spectra of canthaxanthin in: *n*-decane (1), 2-propanol (2) and CS_2 (3).

formed with DPPC displays electronic absorption spectra very different from those recorded in the organic solvents, independently of the physical state of the membrane (Fig. 2). Interestingly, both the main phase transition of DPPC membranes ($P'_\beta \rightarrow L_\alpha$; ~41 °C) as well as the so-called phase pretransition ($L'_\beta \rightarrow P'_\beta$; ~35 °C) almost do not affect the molecular organization of CAN in the lipid phase, that can be seen directly by the electronic absorption spectra of the pigment molecules. The very strong effect of the physical state of the membranes on molecular organization of membrane-bound carotenoids has been reported in the case of other xanthophyll pigments, for example lutein and zeaxanthin [35]. The absorption spectrum of CAN in lipid phase is composed of two distinct bands, one that centers at approximately 490 nm and the second centers at 560 nm or 600 nm, depending on the actual concentration of the carotenoid in the lipid phase. The long-wavelength band appears at 560 nm in most cases except the samples with very low concentration of CAN (below 0.5 mol%, see Fig. 2A). It is very difficult to assign any of these spectral bands to particular molecular organization forms. The main absorption band which centers at ca. 490 nm may be putatively assigned as representing CAN in the monomeric state [5]. On the other hand, this band is considerably broadened in the lipid phase and shifted towards longer wavelengths as compared with the same band of CAN recorded in numerous organic solvents.

Fig. 3 presents the dependence of a position of absorption maximum on a wavenumber scale on the dielectric properties of the chromophore environment, represented by the polarization term, dependent on a refraction index of a solvent [34,36]. As it may be seen, the energies of this particular electronic transition depend not only on dielectric properties of the chromophore environment but also on the fact whether

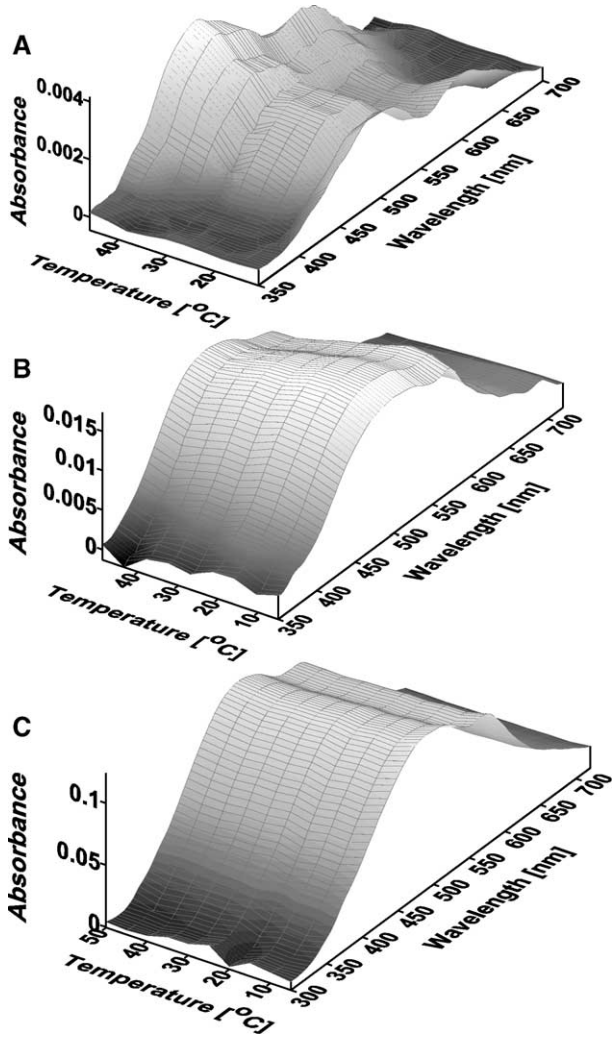

Fig. 2. Temperature dependences of the electronic absorption spectra of DPPC liposomes containing canthaxanthin incorporated at different concentrations with respect to lipid: 0.2 mol% (A), 0.5 mol% (B) and 2 mol% (C).

or not the organic solvents applied are able to form hydrogen bonds with CAN keto groups either directly or indirectly via water molecules. Formally, the keto groups localized at the 4 and 4′ positions extend the conjugated double bonds length. Additional polarization of the chromophore owing to the hydrogen bonding would create a permanent dipole moment able to affect electronic properties of both ground state and the B_u^+ state. In general, the linear dependence on Fig. 3 plotted for the organic solvents able to form hydrogen bonds (solvents 1–6) is shifted towards lower energies (higher wavelengths) as compared to the dependence plotted for other solvents. Assuming that the refractive index of the hydrophobic core of DPPC at 20 °C is 1.49 [37] and corresponding polarization term is 0.289, the position of the absorption maximum of CAN in the lipid phase can be predicted as 20,838 cm^{-1} (480 nm) or 20,321 cm^{-1} (492 nm) in the case of solvents unable and able to form hydrogen bonds respectively, based on the linear dependences. The position of the second absorption maximum corresponds very well to the maximum of the main absorption band of CAN incorporated into liposomes formed with DPPC. The effect of spectral broadening of CAN in the lipid phase reflects most probably the distortions of molecular geometry upon binding to the lipid bilayer, such as torsional deformations about the single C–C bonds [38]. In most cases water molecules are attached to polar groups in the hydrated lipid membranes. Most likely the membrane-bound CAN carry hydrogen-bound water molecules. It is possible that the binding of CAN to the lipid bilayer is associated with the formation of hydrogen bonds, via water bridges, between the keto groups of the carotenoid located at the 4 and 4′ positions and the ester carbonyl groups of the DPPC molecules at two opposite borders of the hydrophobic core of the bilayer. Another possibility is a binding of the pigment into the single lipid monolayer, as postulated in the case of lutein [1,2,39,40]. The binding of the CAN molecule into the lipid bilayer may be associated with a torsion and in particular certain twisting of the terminal β-ionone rings upon the formation of two hydrogen bonds at the opposite sides of the molecule. Since the amplitude of the long-wavelength absorption band of CAN incorporated into liposomes increases with the increase in carotenoid concentration, it is highly probable that this band represents an aggregated form of CAN in the lipid phase. The spectral shift accompanying aggregation and originating from the dipole–dipole interaction of neighboring molecules can be described by the following dependence, within the framework of the exciton-splitting theory [41–43]:

$$v_m = v_{\mathrm{mon}} + 2\beta\cos\left(\frac{m\pi}{N+1}\right) \quad (1)$$

where v_m is the position of the mth excitation state in the spectrum of the aggregated form, v_{mon} is the position of the

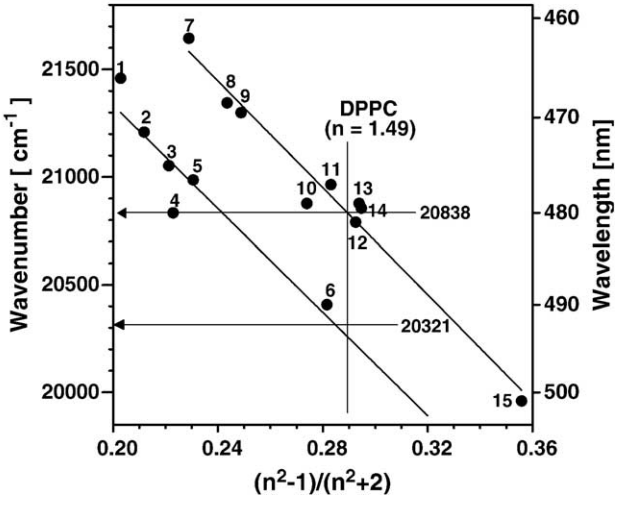

Fig. 3. Position of the absorption maximum of canthaxanthin in different organic solvents versus polarization term expressed as $(n^2-1)/(n^2+2)$; n—refraction index of solvents. Numbers refer to the following solvents: 1—methanol, 2—acetonitrile, 3—acetone, 4—ethanol, 5—isopropanol, 6—DMSO, 7—hexane, 8—refraction oil, 9—n-decane, 10—CCl_4, 11—paraffin, 12—toluene, 13—xylene, 14—benzene, and 15—CS_2. See the text for further explanations.

electronic transition in the spectrum of monomeric chromophores, N is the number of all exciton states (number of aggregate forming molecules) and m is the number of the particular exciton state considered. In formula (1), β is a dipole–dipole coupling matrix element and is expressed as [43]:

$$\beta=\frac{|\mu_{\mathrm{mon}}|^2}{4\pi\varepsilon_0 n^2 R^3}\left(\cos\theta-3\cos^2\phi\right) \quad (2)$$

In the formula, μ_{mon} is the dipole transition moment of a monomer, ε_o is the dielectric permeativity of vacuum, n is the refractive index of the medium and R is the distance between the centers of the transition dipoles of the nearest neighbors in the aggregate, θ is the angle between monomeric transition moment vectors and ϕ is the angle between the transition moment vector and the axis connecting the centers of the transition moment vectors of neighboring molecules. The dipole transition moment of the $1A_g^- \rightarrow B_u^+$ transition of CAN was determined on the basis of integration of the absorption spectrum recorded in ethanol as 15.3 Debye. Assuming that chromophores of CAN in the aggregate are spaced by 1 nm, the distance very close to the spacing of the CAN molecules in the crystallographic structure viewed in the direction of [001] [44], and that all chromophores in the aggregated structure are roughly parallel (θ=0) and additionally taking into consideration the orientation angle of the CAN chromophore in the aggregated state with respect to the axis normal to the membrane (47°, see Table 1), which corresponds to the ϕ angle 43°, one obtains the energy of the dipole–dipole interaction β=−319 cm^{-1}. Such a spectral shift corresponds to the position of the molecular association-related absorption maximum at 20,089 cm^{-1} (498 nm) in the case of dimers or approximately at 19,770 cm^{-1} (506 nm) in the case of an aggregate composed of large number of molecules. Clearly, the bathochromic spectral shifts of CAN in the lipid phase are much larger and cannot be explained in terms of dipole–dipole interactions within the aggregated structures proposed. Assuming closer distance of the carotenoid molecules, for example as close as in the case of molecular packing in the monomolecular layer of CAN formed at the air–water interface, R=0.84 nm, calculated on the basis of specific molecular area (S=0.55 nm^2 [45]) one arrives to β=−538 cm^{-1} and positions of absorption maxima at 19,870 cm^{-1} (503 nm) and 19,332 cm^{-1} (517 nm) for molecular dimers and bulk aggregates respectively. The fact that the orientation angles of CAN in the lipid phase depend on the actual concentration of the pigment may suggest that molecular structures are formed, characterized by chromophores tilted with respect to the axis normal to the plane of the membrane. In the case of monomers of CAN (measurements at 0.5 mol%), the orientation of the transition dipole (20°, see Table 1) suggests roughly the vertical orientation of the axis connecting opposite polar groups of the xanthophyll, taking into consideration the angle between the molecular polarization axis and the axis connecting the keto groups at the 4 and 4′ positions. The thickness of the hydrophobic core of the canthaxanthin-modified DPPC membranes, which can be calculated from the diffractometrically-determined periodicity parameter of the lipid multibilayer (3.2 nm at 40 °C, see Fig. 4), is larger than the distance of the keto groups of CAN (~2.7 nm, [44]). Such a comparison implies the vertical orientation of CAN molecules with respect to the plane of the membrane [1,2].

Table 1
Mean orientation of the transition dipole moment of canthaxanthin, incorporated into the lipid membranes formed with dipalmitoylphosphatidylcholine, with respect to the axis normal to the plane of the membranes

Canthaxanthin content [mol%]	Mean orientation angle [°]±S.D.
0.5	20±3 (3)
2	47±3 (6)

Number of independent experiments in parentheses.

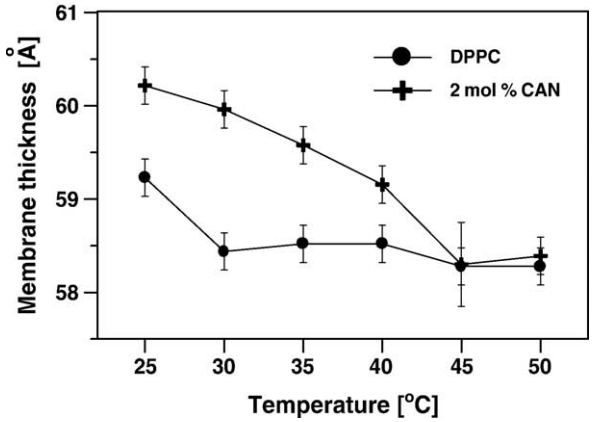

Fig. 4. The temperature profiles of the thickness of DPPC bilayers and bilayers formed with DPPC containing 2 mol% canthaxanthin (CAN) determined diffractometrically as a periodicity of a lipid multibilayer composed of 50 lipid bilayers, deposited to a glass support.

The calculations performed above within the framework of the exciton splitting theory indicate that the formation of molecular aggregates of CAN in the lipid phase accounts for the broadening of the absorption spectra but cannot explain large bathochromic spectral shift observed. Most probably, this effect is directly associated with both exciton interaction and molecular twisting owing to the interaction of CAN with lipids upon binding to the membrane. The end β-rings of CAN have dihedral angles of ca. − 43° [44] and it is highly probable that the involvement of both keto groups in the formation of hydrogen bonding results in twisting of the rings that may induce a spectral shift. Despite the molecular origin of the pronounced bathochromic spectral shift, it is clear that such a shift is specific for CAN incorporated into the lipid membrane and diagnostic for the strong carotenoid–lipid interaction. Such a strong interaction is also pronounced in the X-ray diffractometric measurements presented in Fig. 4. The higher membrane thickness,

observed in the case of the presence of CAN (like in the case of lutein but unlike in the case of zeaxanthin, see discussion elsewhere [2,46]), is indicative of strong interaction between the rigid molecule of CAN and alkyl chains of lipid molecules, which are forced to adopt extended conformation, most probably owing to the van der Waals interactions. On the other hand, the increase in the thickness of the hydrophobic core of the membrane, observed, increases further the disproportions between the thickness of the hydrocarbon core of the bilayers formed with DPPC and the distance between the opposite polar groups of the xanthophyll. Such a disproportion suggests that CAN may adopt also horizontal orientation with respect to the plane of the membrane and remain located in a single lipid monolayer.

The ordering effect of CAN with respect to DPPC membranes emerges also from the analysis of the size of liposomes formed and ^{1}H-NMR spectra of CAN-pigmented liposomes as discussed below. Fig. 5 presents the size dependences of extruded unilamellar liposomes formed with DPPC and EYPC containing different amounts of CAN. Liposomes were prepared at 50 °C and analyzed at 20 °C (below the main phase transition temperature of DPPC) and at 50 °C (above the main phase transition temperature of DPPC). The analysis of the liposome size distribution profiles shows that the incorporation of CAN into the DPPC membranes affects the physical properties of liposomes so that vesicles tend to aggregate. This is demonstrated by the broadening of the distribution profile and, in particular, by the appearance of the second fraction, shifted towards higher diameter values. A liposome aggregation was not observed in the fluid state of the lipid membranes both in the EYPC liposome suspension under the room temperature conditions and in the DPPC liposome suspension incubated at 50 °C (except very high concentration of CAN in the lipid phase, 5 mol%). The molecular mechanism(s) directly involved in the liposome aggregation has to be related to the surface properties of lipid membranes and therefore it is not surprising that the modification of the lipid headgroup region, owing to the CAN incorporation, would affect this phenomenon. On the other hand, it seems interesting that this mechanism is pronounced almost exclusively in the rigid state of the liposome membranes. It is very likely that the molecular motions of lipid molecules in the fluid phase of the membrane and the membrane surface deformations effectively prevent vesicle aggregation. The stabilizing effect of CAN on the lipid headgroup region may also restrict this kind of molecular motions and prevent surface deformations.

In order to understand in more detail the molecular mechanisms responsible for the organization of canthaxanthin-containing lipid membranes, the ^{1}H-NMR spectra of pigmented DPPC liposomes were recorded and analyzed. Praseodymium ions were added to each sample before spectrum recording in order to analyze molecular packing phenomena in the lipid headgroup region according to the methodology applied previously while analyzing lipid membranes modified with β-carotene and zeaxanthin [33]. Figs. 6A and B present CAN concentration dependence of the full width at half height of the ^{1}H-NMR maximum corresponding to the CH_2 groups and CH_3 groups of alkyl chains of EYPC, respectively, that appear at characteristic chemical shift values of 1.36 ppm (CH_2) and 1.07 ppm (CH_3). As may be seen in both cases, the presence of CAN broadens the resonance maxima, which is a demonstration of a restriction to the segmental molecular motions [33,47]. The maximum effect of CAN in the case of CH_2 groups (the increase in the width by 86%) and in the case of CH_3 groups (the increase in the width by 72%) is not as strong as in the case of zeaxanthin, where the increase in the width was higher than 220% for CH_2 groups as well as for CH_3 groups [33]. On the other hand, at a relatively low concentration of a carotenoid in the lipid phase (below 1 mol%), the effect of CAN is ca. twice as strong as in the case of zeaxanthin in the case of both groups. An abrupt change in the dependence corresponding to the CH_2 groups (Fig. 6A), just above 1 mol% CAN in the lipid phase, corresponds most probably to the threshold concentration, above which the formation of molecular structures (e.g. dimers) takes place. Such an explanation has also strong support from the difference in the orientation of CAN in the lipid membranes at concentrations higher and lower than 1 mol% (see Table 1). The restriction of the segmental molecular motion of the CH_2 and terminal CH_3 groups forming the hydrophobic core of the lipid bilayer can be explained in terms of van der Waals interactions between the rigid rod-like molecules of the carotenoid and alkyl chains of the lipid molecules undergoing very fast gauche-trans isomerization. Interestingly, a relatively sharp transition in the molecular motion of lipid headgroup, as monitored by the width at half height of the ^{1}H-NMR resonance of the $-N^+(CH_3)_3$ group (3.42 ppm), is observed between the CAN concentrations 1 mol% and 1.5 mol% (Fig. 6C). Such an effect shows that an increase in the CAN concentration in the lipid phase, in the range below the aggregation threshold, increases order within the hydrophobic core (Figs. 6A and B) but at the same time, even the opposite effect can be observed in the headgroup region, most probably owing to the increase in the distance between the lipid molecules. It is not clear why the formation of molecular associates, such as dimers, at the CAN concentrations above 1 mol% would exert certain restrictions to molecular motion in the polar headgroup region. It is also possible that, such as in the case of lutein [1,2,31,35,40,46], a certain fraction of CAN adopts horizontal orientation with respect to the plane of the lipid bilayer and links different polar lipid heads via hydrogen bonding. The coexistence of two roughly orthogonal orientation fractions of CAN can also explain the bigger angle between the transition dipole of the carotenoid and the axis normal to the plane of the membrane, determined at 2 mol% (47°) as compared to that determined at 0.5 mol% of carotenoid (20°). Fig. 7A presents the effect of the addition of praseodymium ions on the ^{1}H-NMR spectrum. This effect consists in a splitting

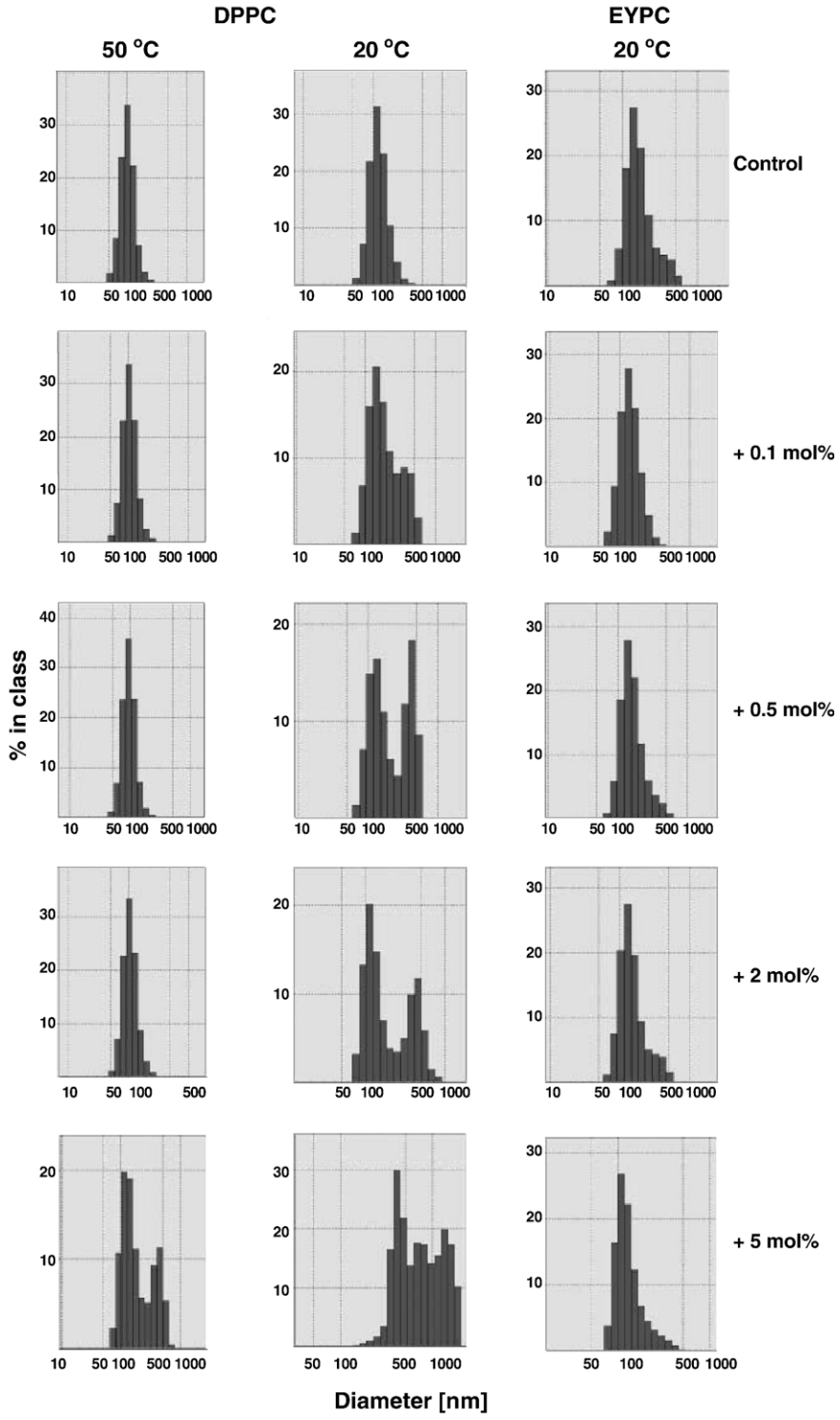

Fig. 5. Size dependency profiles of DPPC liposomes determined at 20 °C and at 50 °C and of EYPC liposomes determined at 20 °C, containing different amount of canthaxanthin, indicated.

of the maximum corresponding to the $-N^{+}(CH_3)_3$ group, caused by the pseudocontact shifts produced by shift reagents (Pr^{3+}) [48]. It appears that this shift (δ) depends on the actual concentration of CAN in the membrane. As it may be seen, an effect of CAN is very low at the concentrations below 1 mol%, but a considerable decrease in the accessibility of Pr^{+3} can be observed at concentrations higher than 1 mol%. Such an effect corroborates with the effect of CAN on the motional freedom of the choline group (Fig. 6C). Fig. 7B presents the CAN concentration dependence of the intensity of Pr^{+3} ion-split resonance maximum corresponding to the $N^{+}(CH_3)_3$ group. The intensity ratio

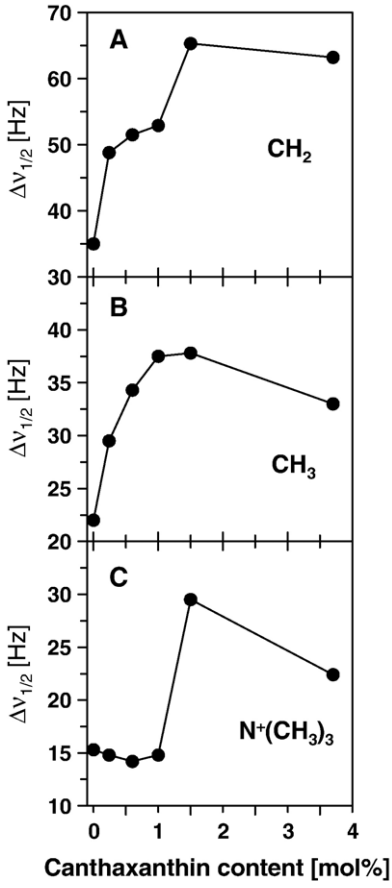

Fig. 6. Canthaxanthin concentration dependences of full width at a half intensity of the ^{1}H-NMR resonance maximum corresponding to (A) CH_2 and (B) CH_3 groups of alkyl chains and (C) $N^+(CH_3)_3$ choline polar headgroups of DPPC in liposomes.

I_{out}/I_{in} above 1.2, typical of the preparation of small unilamellar liposomes [33], expresses the number of lipid molecules in the outer monolayer of the bilayer relative to the number of lipid molecules in the inner monolayer of liposomes. A decrease in the ratio below 1, accompanying the increase in the concentration of CAN, reflects vesicle aggregation in the preparation subjected to ^{1}H-NMR experiments, before exposition to Pr^{+3} ions. The same effect was observed in the photon correlation-light scattering experiments, as discussed above.

In order to get more detailed information concerning molecular mechanisms of interaction of CAN with lipid molecules at low and at higher concentration of the carotenoid, the pigmented liposomes were deposited to a ZnSe crystal in the form of oriented lipid multibilayers and analyzed by means of ATR-FTIR technique. Fig. 8 presents the infrared absorption spectra of the samples composed of pure DPPC and DPPC with 0.5 or 2 mol% CAN, in the region between 800 and 2000 cm^{-1}. The Van der Waals interactions of CAN and alkyl chains of a lipid, responsible for the membrane rigidifying effect, as concluded from the results of the ^{1}H-NMR measurements, are also manifested in the FTIR spectra. In particular, the position of the band corresponding to the scissoring vibrations of the CH_2 groups of alkyl chains (1470 cm^{-1} [49]) is shifted by 3 cm^{-1} towards lower wavenumbers upon the incorporation of CAN into the membranes. Apart from the spectral shift, the band becomes more narrow, which is an indication of the ordering effect of CAN with respect to the hydrocarbon membrane core. Interestingly, the most pronounced effects of CAN on the infrared absorption spectrum of the DPPC membranes are visible in the bands representing the vibrations of functional groups located in the lipid bilayer headgroup region. In particular, the band that centers at 1068 cm^{-1}, assigned to the C–O–P–O–C stretching vibrations [49], is very sensitive to the presence of CAN. The position of this peak becomes shifted to lower wavenumbers by almost 20 cm^{-1} upon binding CAN into the membranes. Such a strong effect suggests the location of at least a certain fraction of the pigment, in the polar headgroup region. Contrary to the phosphodiester backbone, the choline group is almost insensitive to the presence of CAN within the membranes. The band at 968 cm^{-1}, assigned to the antisymmetric stretching vibrations of the $N^+(CH_3)_3$ group, remains virtually at the same position in the control and carotenoid-containing samples. Such a difference suggests the binding of a certain fraction of CAN to a single monolayer of the lipid bilayer and pigment orientation stabilized via hydrogen bonding to the lipid phosphatidyl groups. Such an interpretation is further

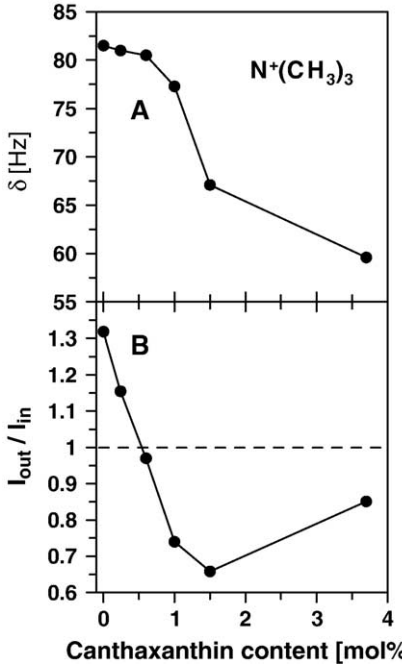

Fig. 7. Canthaxanthin concentration dependences of (A) the distance between the ^{1}H-NMR resonance maxima corresponding to $N^+(CH_3)_3$ choline polar headgroups of DPPC in liposomes, split after the addition of $PrCl_3$ and (B) intensity ratio (I_{out}/I_{in}) of the upfield and downfield ^{1}H-NMR resonance maxima, related to the outer and inner lipid monolayers of the liposome membranes, respectively.

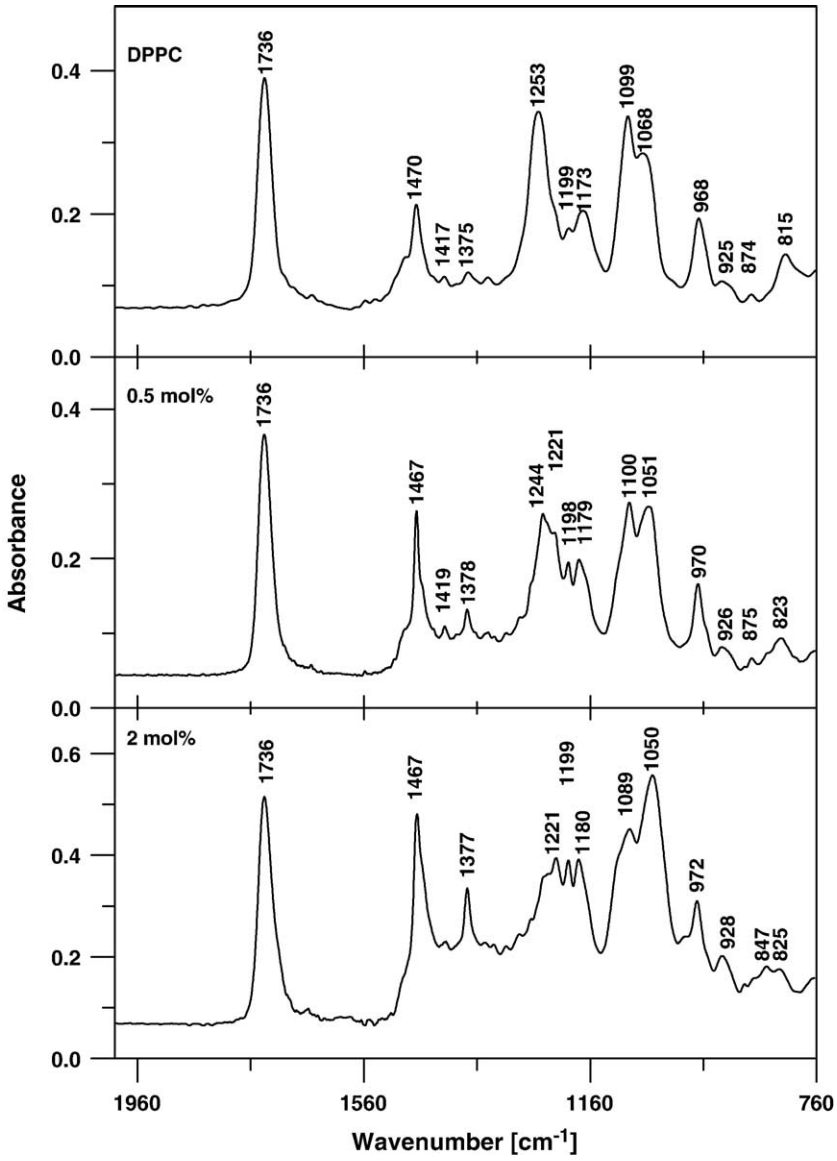

Fig. 8. FTIR spectra of DPPC liposomes deposited to ZnSe crystal as a lipid multibilayer, pure (upper panel) or containing incorporated canthaxanthin at 0.5 mol% and 2.0 mol%, indicated. Positions of selected absorption maxima are marked.

supported by the analysis of the position of spectral bands corresponding to the symmetric and antisymmetric stretching vibrations of PO_2^- groups (at 1099 cm^{-1} and at 1253 cm^{-1} respectively in the pure DPPC membrane). These bands become shifted towards lower wavenumbers by 10 cm^{-1} and 30 cm^{-1}, respectively, in the membranes containing 2 mol% CAN, which is indicative of the immobilization of this fragment of the lipid molecule, presumably due to a hydrogen bond formation. The detailed analysis of the FTIR spectra of DPPC membranes containing 2 mol% CAN in the region corresponding to the carbonyl group vibration (Fig. 9) reveals that the incorporation of the xanthophyll is associated with the appearance of the new spectral bands. The band corresponding to the stretching vibration of the keto groups of pure CAN is located at 1657 cm^{-1} in the KBr environment [50]. This band is observed in the difference spectrum at 1659 cm^{-1} and represents the keto groups of CAN incorporated into the membrane. Another broad band in the difference spectrum, with the maximum at 1588 cm^{-1}, can be assigned to the C═C stretching vibrations of the membrane-bound carotenoid pigment [50]. The main band corresponding to the ester carbonyl group stretching vibrations of lipids (that centers at 1736 cm^{-1}) is also affected by the incorporation of CAN into the membranes. It can be observed, the appearance of the new spectral component of the principal band at 1712 cm^{-1} and concomitant disappearance of the band at 1751 cm^{-1}. The fact that the negative band appears in the difference spectrum at the higher-wavenumber edge of the main band corresponding to the ester carbonyl group vibrations indicates that a certain pool of DPPC molecules interact with CAN via the lipid ester carbonyl groups.

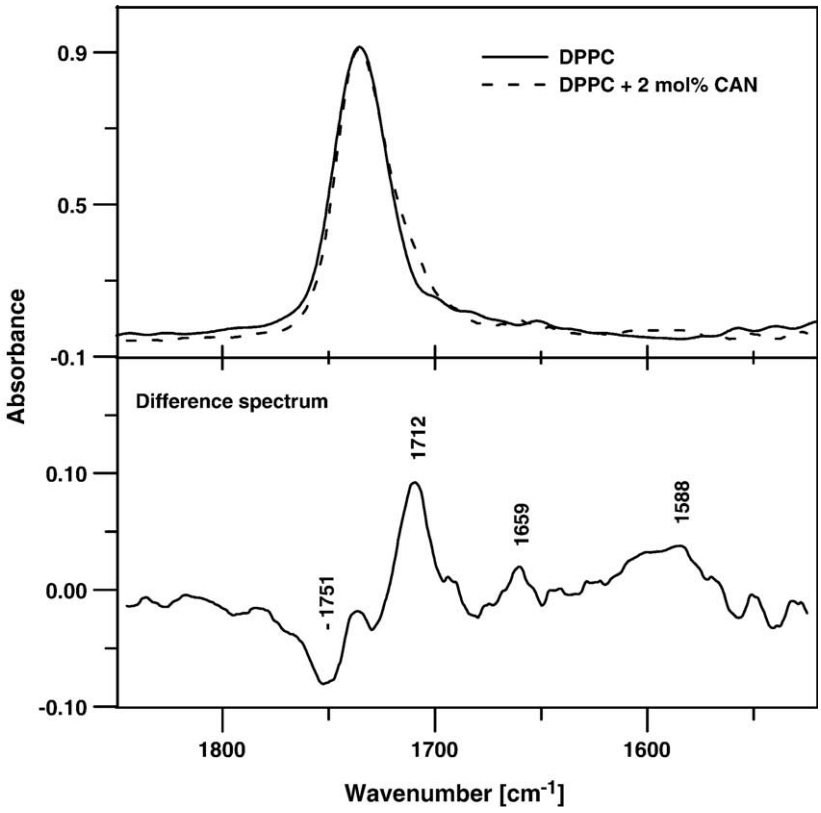

Fig. 9. Normalized FTIR spectra, presented in the region corresponding to the carbonyl group vibrations, of DPPC liposomes deposited to ZnSe crystal as a lipid multibilayer, pure and containing incorporated 2.0 mol% canthaxanthin (upper panel) and the difference spectrum (lower panel) of DPPC+CAN minus DPPC.

Owing to these interactions, the components of the main C═O spectral band, representing the lipid molecules interacting with CAN, are shifted towards lower wavenumbers. The analysis of the FTIR spectra confirms also the diversity of localization as well as possible molecular interactions of CAN with lipids in the membranes. The spectral analysis shows that the effect of CAN on the polar headgroup region is much more pronounced. It is therefore possible that the fraction of CAN molecules localized entirely in the polar headgroup region is particularly active in the modification of the structural and dynamic properties of lipid membranes.

Both carotenoid incorporation to lipid membranes and an effect on dynamic and structural properties of membranes depend on their actual composition. In particular, a presence of other modifying molecules, such as cholesterol and other carotenoids, and a presence of membrane proteins may modulate the effect of CAN on the physical properties of biomembranes. In the present work, we applied a liposome model system to focus our research on the specific mechanisms responsible for the molecular interactions of CAN and lipids. Despite this limitation, all the results of the experiments described in this work point into very strong effect of CAN on the physical properties of lipid membranes. Comparing to the other xanthophyll pigments analyzed previously, the striking difference is that the effects of CAN at a molecular level are observed at relatively low concentration of the pigment in the lipid phase (even below 2 mol%).

Acknowledgements

Thanks are due to Dr. Jerzy Gubernator for his expertise guiding in the PCS measurements. This work was supported by the Ministry of Scientific Research and Information Technology of Poland from the budget founds for science in the years 2004–2007 within the research project 2P05F04327 and by the grant to Agricultural University in Wroclaw and to Jagiellonian University in Krakow No. 158/E-338-/SPUB-M/5 PR UE/DZ 9/2001–2003.

References

[1] W.I. Gruszecki, Carotenoid orientation: role in membrane stabilization, in: N.I. Krinsky, S.T. Mayne, H. Sies (Eds.), Carotenoids in Health and Disease, Marcel Dekker, New York, 2004, pp. 151–163.
[2] W.I. Gruszecki, Carotenoids in membranes, in: H.A. Frank, A.J. Young, G. Britton, R.J. Cogdell (Eds.), The Photochemistry of Carotenoids, Kluwer Academic Publ., Dordrecht, 1999, pp. 363–379.
[3] H.A. Frank, J.A. Bautista, S.J. Josue, A.J. Young, Mechanism of nonphotochemical quenching in green plants: energies of the lowest

excited singlet states of violaxanthin and zeaxanthin, Biochemistry 39 (2000) 2831–2837.
[4] G. Britton, Structure and properties of carotenoids in relation to function, FASEB J. 9 (1995) 1551–1558.
[5] G. Britton, S. Liaaen-Jensen, H. Pfander, Carotenoids Handbook, Birkhauser Verlag AG, Basel, 2004.
[6] A.K. Gupta, H.F. Haberman, D. Pawlowski, G. Shulman, I.A. Menon, Canthaxanthin, Int. J. Dermatol. 24 (1985) 528–532.
[7] N.I. Krinsky, Carotenoid protection against oxidation, Pure Appl. Chem. 51 (1979) 649–660.
[8] N.I. Krinsky, J.T. Landrum, R.A. Bone, Biologic mechanisms of the protective role of lutein and zeaxanthin in the eye, Annu. Rev. Nutr. 23 (2003) 171–201.
[9] N.I. Krinsky, K.J. Yeum, Carotenoid–radical interactions, Biochem. Biophys. Res. Commun. 305 (2003) 754–760.
[10] H. Sies, W. Stahl, Carotenoids and UV protection, Photochem. Photobiol. Sci. 3 (2004) 749–752.
[11] W. Stahl, H. Sies, Antioxidant activity of carotenoids, Mol. Aspects Med. 24 (2003) 345–351.
[12] C.W. Lober, Canthaxanthin—The “tanning” pill, J. Am. Acad. Dermatol. 13 (1985) 660.
[13] B.P. Chew, J.S. Park, M.W. Wong, T.S. Wong, A comparison of the anticancer activities of dietary beta-carotene, canthaxanthin and astaxanthin in mice in vivo, Anticancer Res. 19 (1999) 1849–1853.
[14] K. Macdonald, G. Holti, J. Marks, Is there a place for beta-carotene/canthaxanthin in photochemotherapy for psoriasis? Dermatologica 169 (1984) 41–46.
[15] G. Wennersten, Carotenoid treatment for light sensitivity: a reappraisal and six years’ experience, Acta Derm.-Venereol. 60 (1980) 251–255.
[16] R. McGuinness, P. Beaumont, Gold dust retinopathy after the ingestion of canthaxanthin to produce skin-bronzing, Med. J. Aust. 143 (1985) 622–623.
[17] B. Daicker, K. Schiedt, J.J. Adnet, P. Bermond, Canthaxanthin retinopathy. An investigation by light and electron microscopy and physicochemical analysis, Graefe Arch. Clin. Exp. Ophthalmol. 225 (1987) 189–197.
[18] C. Harnois, J. Samson, M. Malenfant, A. Rousseau, Canthaxanthin retinopathy. Anatomic and functional reversibility, Arch. Ophthalmol. 107 (1989) 538–540.
[19] G.L. White Jr., R. Beesley, S.M. Thiese, R.T. Murdock, Retinal crystals and oral tanning agents, Am. Fam. Phys. 37 (1988) 125–126.
[20] A.M. Ros, H. Leyon, G. Wennersten, Crystalline retinopathy in patients taking an oral drug containing canthaxanthin, Photodermatology 2 (1985) 183–185.
[21] G.B. Arden, J.O. Oluwole, P. Polkinghorne, A.C. Bird, F.M. Barker, P.G. Norris, J.L. Hawk, Monitoring of patients taking canthaxanthin and carotene: an electroretinographic and ophthalmological survey, Hum. Toxicol. 8 (1989) 439–450.
[22] S. Bopp, E.L. el-Hifnawi, H. Laqua, Canthaxanthin retinopathy and macular pucker, J. Fr. Ophtalmol. 12 (1989) 891–896.
[23] G. Boudreault, P. Cortin, L.A. Corriveau, A.P. Rousseau, Y. Tardif, M. Malenfant, Canthaxanthin retinopathy: 1. Clinical study in 51 consumers, Can. J. Ophthalmol. 18 (1983) 325–328.
[24] U. Weber, W. Kern, G.E. Novotny, G. Goerz, S. Hanappel, Experimental carotenoid retinopathy: I. Functional and morphological alterations of the rabbit retina after 11 months dietary carotenoid application, Graefe Arch. Clin. Exp. Ophthalmol. 225 (1987) 198–205.
[25] U. Weber, G. Goerz, H. Baseler, L. Michaelis, Canthaxanthin retinopathy. Follow-up of over 6 years, Klin. Monatsbl. Augenheilkd. 201 (1992) 174–177.
[26] R. Hennekes, Peripheral retinal dystrophy following administration of canthaxanthin? Fortschr. Ophthalmol. 83 (1986) 600–601.
[27] R. Bluhm, R. Branch, P. Johnston, R. Stein, Aplastic anemia associated with canthaxanthin ingested for ‘tanning’ purposes, JAMA 264 (1990) 1141–1142.
[28] J.A. Oosterhuis, H. Remky, N.M. Nijman, A. Craandijk, F.A. de Wolff, Canthaxanthin retinopathy without intake of canthaxanthin, Klin. Monatsbl. Augenheilkd. 194 (1989) 110–116.
[29] R. Goralczyk, S. Buser, J. Bausch, W. Bee, U. Zuhlke, F.M. Barker, Occurrence of birefringent retinal inclusions in cynomolgus monkeys after high doses of canthaxanthin, Investig. Ophthalmol. Vis. Sci. 38 (1997) 741–752.
[30] R. Goralczyk, F.M. Barker, S. Buser, H. Liechti, J. Bausch, Dose dependency of canthaxanthin crystals in monkey retina and spatial distribution of its metabolites, Investig. Ophthalmol. Vis. Sci. 41 (2000) 1513–1522.
[31] A. Sujak, W. Okulski, W.I. Gruszecki, Organisation of xanthophyll pigments lutein and zeaxanthin in lipid membranes formed with dipalmitoylphosphatidylcholine, Biochim. Biophys. Acta 1509 (2000) 255–263.
[32] D. Rengel, A. Diez-Navajas, A. Serna-Rico, P. Veiga, A. Muga, J.C. Milicua, Exogenously incorporated ketocarotenoids in large unilamellar vesicles. Protective activity against peroxidation, Biochim. Biophys. Acta 1463 (2000) 179–187.
[33] J. Gabrielska, W.I. Gruszecki, Zeaxanthin (dihydroxy-beta-carotene) but not beta-carotene rigidifies lipid membranes: a 1H-NMR study of carotenoid-egg phosphatidylcholine liposomes, Biochim. Biophys. Acta 1285 (1996) 167–174.
[34] W.I. Gruszecki, J. Sielewiesiuk, Orientation of xanthophylls in phosphatidylcholine multibilayers, Biochim. Biophys. Acta 1023 (1990) 405–412.
[35] A. Sujak, W.I. Gruszecki, Organization of mixed monomolecular layers formed with the xanthophyll pigments lutein or zeaxanthin and dipalmitoylphosphatidylcholine at the argon–water interface, J. Photochem. Photobiol., B Biol. 59 (2000) 42–47.
[36] P.O. Andersson, T. Gilbro, L. Fergusson, Absorption spectral shifts of carotenoids related to medium polarizability, Photochem. Photobiol. 54 (1991) 353–360.
[37] M. Gagos, R. Koper, W.I. Gruszecki, Spectrophotometric analysis of organisation of dipalmitoylphosphatidylcholine bilayers containing the polyene antibiotic amphotericin B, Biochim. Biophys. Acta 1511 (2001) 90–98.
[38] S. Krawczyk, D. Olszowka, Spectral broadening and its effect in Stark spectra of carotenoids, Chem. Phys. 265 (2001) 335–347.
[39] A. Sujak, J. Gabrielska, W. Grudzinski, R. Borc, P. Mazurek, W.I. Gruszecki, Lutein and zeaxanthin as protectors of lipid membranes against oxidative damage: the structural aspects, Arch. Biochem. Biophys. 371 (1999) 301–307.
[40] W.I. Gruszecki, A. Sujak, K. Strzalka, A. Radunz, G.H. Schmid, Organisation of xanthophyll-lipid membranes studied by means of specific pigment antisera, spectrophotometry and monomolecular layer technique lutein versus zeaxanthin, Z. Naturforsch., C 54 (1999) 517–525.
[41] M. Kasha, Energy transfer mechanisms and the molecular exciton model for molecular aggregates, Radiat. Res. 20 (1963) 55–71.
[42] M. Kasha, H.R. Rawls, M. Ashraf El-Bayoumi, The exciton model in molecular spectroscopy, Pure Appl. Chem. 11 (1965) 371–392.
[43] J. Parkash, J.H. Robblee, J. Agnew, E. Gibbs, P. Collings, R.F. Pasternack, J.C. de Paula, Depolarized resonance light scattering by porphyrin and chlorophyll a aggregates, Biophys. J. 74 (1998) 2089–2099.
[44] J.C.J. Bart, C.H. MacGillavry, The crystal and molecular structure of canthaxanthin, Acta Crystallogr. B24 (1968) 1587–1606.
[45] J. Sielewiesiuk, K. Veeranjaneyulu, R.M. Leblanc, Cryptoxanthin, echinenone and hydroxyechinenone films at the air–water interface, Ann. UMCS Sectio AAA 57 (2002) 123–135.
[46] A. Sujak, P. Mazurek, W.I. Gruszecki, Xanthophyll pigments lutein and zeaxanthin in lipid multibilayers formed with dimyristoylphosphatidylcholine, J. Photochem. Photobiol., B Biol. 68 (2002) 39–44.
[47] I. Jezowska, A. Wolak, W.I. Gruszecki, K. Strzalka, Effect of beta-carotene on structural and dynamic properties of model phosphati-

dylcholine membranes: II. A 31P-NMR and 13C-NMR study, Biochim. Biophys. Acta 1194 (1994) 143–148.
[48] G. Royden, A. Hunt, L.R.H. Tipping, *Trans*-bilayer pseudocontact shifts produced by lanthanide Ions in the 1H- and 31P-NMR spectra of phospholipids, vesicular membranes and their temperature variation, J. Inorg. Biochem. 12 (1980) 17–36.
[49] L.K. Tamm, S.A. Tatulian, Infrared spectroscopy of proteins and peptides in lipid bilayers, Q. Rev. Biophys. 30 (1997) 365–429.
[50] K. Bernhard, M. Grosjean, Infrared spectroscopy, in: G. Britton, S. Liaaen-Jensen, H. Pfander (Eds.), Carotenoids, Spectroscopy, vol. 1B, Birkhauser Verlag, Basel, 1995, pp. 117–134.